Journal of Applied Fluid Mechanics, Vol. 13, No. 2, pp. 549-559, 2020.
Available online at www.jafmonline.net, ISSN 1735-3572, EISSN 1735-3645.
DOI: 10.29252/jafm.13.02.30218

Time Domain Simulation of Ship Motion in Irregular Oblique Waves

S. M. Mousavi[1†], A. R. Khoogar[2] and H. Ghasemi[3]

[1] *Maritime Engineering Department, Malek Ashtar University of Technology*
[2] *Mechanical Engineering Department, Malek Ashtar University of Technology*
[3] *Marine Engineering Department, Amirkabir University of Technology*

†*Corresponding Author Email: srmousavi@aut.ac.ir*

(Received March 2, 2019; accepted July 12, 2019)

ABSTRACT

Ship harmonic motion is an important and practical characteristic in ship design and performance evaluation. The development and optimization of hull-form, ship's dynamic effects, seakeeping performance, and motion control, all require the motion data that includes wave exciting forces as well as dynamic response of the ship. This paper presents a new approach for time-domain simulation of full-scale ship model with four degrees of freedom based on computational fluid dynamics using unsteady RANS method. The key objective of this paper was the full-scale simulation of ship motion in oblique waves and assessment of time domain forces, moments, and other motion parameters. The David Taylor Model Basin (DTMB) 5415 full-scale model has been used for the numerical studies in this paper. The obtained computational results showed good conformation to the results obtained using the strip theory. It is intended to extend this research to subscale test experiments for more definite validation of the results.

Keywords: Ship full-scale; CFD; DTMB5415; Irregular wave; Seakeeping; Roll motion.

NOMENCLATURE

CF	Correction Factor
G	Grid
GCI	Grid Convergence Factor
H	significant height of oscillation
RG	convergence ratio in grid uncertainty study
rG	refinement ratio of grids
RMS	Route Mean Square
RT	convergence ratio in time-step uncertainty study
rT	refinement ratio of time-step
Sc	corrected solution
S_{Gi}	Solution for grid type i
S_{Ti}	Solution for time-step type i
T	oscillation period
Te	encounter oscillation period
U	uncertainty / flow velocity
UG	grid uncertainty
UGc	corrected grid uncertainty
u_i	velocity in i direction
UT	time-step uncertainty
UTc	corrected time-step uncertainty
δ	solution error / Kronecker delta function
Δt	time step
Δx	mesh cell dimension
μ	viscosity / wave direction
ω	oscillation frequency
ω_e	oscillation encounter frequency

1. INTRODUCTION

In many cases, commercial ships in their passage or naval vessels in their mission encounter storms and rough sea conditions. During such circumstances, ships try to obtain the best seakeeping performance so as to reduce speed or changing direction; in order to reduce the dynamic effects like slamming or propeller emergence. The improvement of seakeeping performance is one of the most important concerns of designers in the preliminary stage of ship design. In naval vessels, the operational capability of equipment highly depends on the dynamic behavior of the vessel. Three principal oscillating ship motions considered in seakeeping studies include: rotational motion about the longitudinal axis referred to as "roll", rotational motion about the transverse axis referred to as

"pitch" and vertical motion along the vertical axis referred to as "heave". Over the last five decades, three-dimensional potential flow theory-based methods have extensively been used to calculate the seakeeping performance of ships. Besides the theoretical methods, experimental model tests extensively is used for seakeeping evaluation and verification of ship designs.

Both methods, that is, the potential flow theory-based method and the seakeeping experimental test, provide good estimates for the heave and pitch responses. Viscous effects such as breaking waves and turbulence are ignored in potential theory, while these effects have a great impact on roll motion.

Also, most marine experimental test facilities in the world make use towing tank for seakeeping test; which only head sea waves can be generated, so the roll motion does not occur. Furthermore, in seakeeping tests, usually the exciting force and moment characteristics are not readily available, and only the dynamic responses are recorded.

Roll motion plays a significant role in the operational capability of naval vessels, the comfortability of passenger vessels, and safety of cargo vessels. Roll amplitude and frequency have adverse effects on many of the onboard equipment such as weapons and the comfort of the crew and passengers. Since 1980 and more so in recent years, several provisions have been used to reduce the adverse impact of roll motion, for example, rudder roll stabilizer or onboard stabilizer tank. Research on hull-form optimization, ship's dynamic effects, seakeeping performance, and motion control all require motion data that includes the exciting forces as well as the dynamic response of the ship.

In recent years, computational fluid dynamic (CFD) software have gained a considerable amount of improvement for ship hydrodynamic simulations. The ultimate goal of such software is usually to increase simulation accuracy and provide a near real-world sea environment, numerically. With great advances made in computers, more sophisticated Reynolds-Averaged Navier-Stokes (RANS) codes have been developed along with more realistic simulations. These advances are well documented in the literature on CFD techniques likes Kodama *et al.* (1994), Larsson *et al.* (2003) and Hino *et al.* (2005).

Gui *et al.* (2002) used RANS to evaluate unsteady resistance, heave force, pitch moment, and free-surface elevations in steady forward speed and regular head waves for a scaled model. Their results were validated using the IIHR towing tank testing. Also, the above situation was compared in the head waves with different steepness and Froude numbers.

Bhushan *et al.* (2007) worked on turbulence modeling and extended the unsteady Reynolds averaged Navier-Stokes. They illustrated that using wall-functions reduce the number of grids near the wall. Based on their results, the multilayer model is accurate and has fewer limitations.

Hanninen *et al.* (2006) compared several computational cases with different RANS methods using full and sub-scale models. The results showed that the Reynolds number has an important effect on the computations. The results also demonstrated that more attention should be given to grids to obtain fully grid independent solutions. The pressure predictions seem to be particularly sensitive to grid resolution.

Alessandrini *et al.* (2008) simulated 6 DOF of ship hull in nonlinear regular head waves under viscous flow theory. A comparison of their simulation results was made for the DTMB-5512 model by IIHR towing tank test.

Simonsen *et al.* (2013) discussed the ignored viscous effects like the wave breaking, turbulence, and damping forces in potential theory and emphasized that in the RANS CFD method, these effects are directly considered.

Tezdogan *et al.* (2015) used the RANS equation to simulate ship responses and the added resistance of a container ship model. Validation of the results was made against available experimental data. The analyses were conducted by utilizing the commercial URANS solver, Star-CCM. The paper investigated ship behavior at an off-design speed and showed that slow steaming of a ship leads to the decrease in the effective power consumption and consequently decrease CO2 emission.

Tezdogan *et al.* (2016) calculated the heave motions of a ship encountering regular head sea waves, by utilizing a RANS solver, Star-CCM. In the paper, simulation of ship roll motion in oblique waves has been suggested as future work.

Mancini *et al.* (2018) simulate roll decay at zero speed and initial roll of 19.58 deg. in calm water. For DTMB5415 Benchmark scaled model. URANS solver, Star-CCM is used for numerical simulation. Simulation was verified using Grid Convergence Index (GCI) method. In this work verification study carried out to investigate the grid and time step uncertainties and simulation results validated by experimental data. In the same article, Gocke *et al.* (2018) simulate roll decay of the DTMB5415 scaled-model with the bilge keel in forwarding speed and calm water. Simulation results were validated using experimental data.

Kianejad *et al.* (2019) using the CFD method to simulate full-scale and model-scale of a post-Panama container ship. In their work roll motion coefficients, especially added mass coefficient, were investigated. Regular wave considered for numerical modeling. Roll added mass results were compared with Bhattacharyya's method. The number of overset mesh and verification study are a useful guide for similar works.

During this research, the numerical results for regular head sea waves are outstanding, while, as suggested in previous studies, this paper aims to develop the current knowledge by calculating the vertical and roll motions of a ship against oblique seas in irregular waves, utilizing the URANS

solver, Star-CCM 10.06.

In most researches, the ship model is fixed in the computational domain while the flow field moves around the ship. Therefore, the vessel speed is set in the inlet boundaries. This type of modeling is applicable to the simulation of the hydrodynamic resistance in calm waters because the model is following the real physics of the problem. But the approach is not appropriate for ship motion simulation in waves, because the waves and ship heading speed are both specified in the inlet boundary. In this type of modeling, the wave energy is damped in the flow field and the wave amplitudes decrease along with the computational domain. This type of modeling is similar to a flow channel with a current speed in which any disturbance in the free surface disappears faster than that in still water. Usually, in the real sea environment, the current speed is negligible and relatively small in comparison with the ship's speed. In this paper, as a novelty, the computational domain is considered similar to the towing tank and irregular waves are generated on the inlet boundary. These waves propagate along with the computational domain while the ship moves ahead in the domain. The four degrees of freedom considered in this study include the ship surge, roll, pitch, and heave. Another advantage of this type of modeling is that it can be used for oblique or non-head sea wave simulations.

In this paper, a CFD simulation of a ship sailing in the seaway, using the commercial RANS solver, Star-CCM, is presented. The novelty and main objective of this research is the simulation of actual ship motion in the real seaway with the following assumptions.

Full-scale ship model.

Four degrees of freedom simulation.

Irregular wave condition.

Sailing through oblique waves.

The possibility of full-scale ship motion modeling with the RANS equations is one of the great advantages of CFD. Dynamic mesh generation, turbulence modeling, free surface modeling and simultaneous solutions to dynamic equations are as well readily possible.

2. CASE STUDY MODEL AND CONDITION

The David Taylor Model Basin (DTMB) 5415 full-scale model is used as a case study in this paper. Figure 1 presents the side view of the 3D model geometry. This model was used in the early 1980s as a preliminary design for a surface combatant. It is one of the benchmark models for ship hydrodynamics, and has been studied extensively, both experimentally and numerically. It has also been used for software validation at Ship Hydrodynamics CFD Workshops in Gothenburg in 2000 (Larsson *et al.* 2003) and Tokyo in 2005 (Hino *et al* 2005).

Fig. 1. DTMB 5415 3D model geometry.

Some experimental data of the scaled model of this ship have published in the literature, and the full-scale model date is presented in Table 1.

Table 1 Case study model data (Toxopeusa *et al.* 2011)

Particular, units	Symbol	Value
Length overall, m	LOA	153.230
Breadth max molded, m	BMAX	20.546
Breadth molded on WL, m	BWL	19.060
Draught molded on FP, m	TF	6.150
Draught molded on AP, m	TA	6.150
Displacement, m^3	Δ	8431.800
Wetted surface area, m^2	S	2972.600
LCB, m (Position aft of FP)	FB	71.970
metacentric height, m	GMt	1.950
VCG, m	KG	7.510
Natural period of roll, s	Tφ	11.500
Block coefficient	CB	0.507
Cruise Speed, m/s	Vc	9.2592
Max Speed, m/s	Vm	15.432

This work aims to simulate the full-scale, 5415 model, heading in oblique irregular waves. Simulations are performed in 170 and 175 degrees of heading angles with the ship design speed. Irregular waves are generated using JONSWAP spectra, and wave parameters include the significant height and modal period. These parameters are selected in accordance with the sea state of 5 referred to in the Pierson-Moskowitz (1963) sea state table. As shown in Fig. 2, a rectangular computational domain is considered for the simulation, and the deflection angle between the domain and the ship model provides the proper heading angle for the ship. Long crest irregular waves are parallel to the inlet boundary of the domain and are propagated along with the domain. Table 2 presents the simulation conditions.

Table 2 Simulation conditions

Heading Speed (knot)	Heading Angle (Degree)	Irregular waves parameter	
		Significant wave height (m)	Modal Period (s)
20	170	3.28	9.146
20	175	3.28	9.146

The length of the computational domain is selected such that the simulation time lasts for 75 seconds. During the CFD calculations, in addition to position, velocity and acceleration of the roll, pitch and heave motions, the exciting forces and moments are also recorded. Recording of the exciting forces and moments in seakeeping tests are

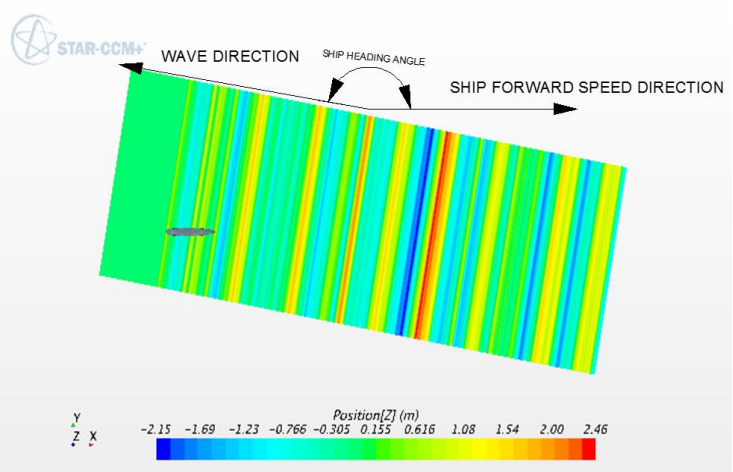

Fig. 2. Computational domain and heading angle.

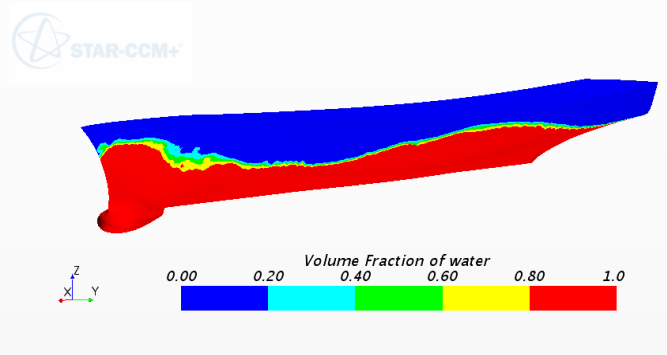

Fig. 3. Value of volume fraction on the ship hull (Fr=0.275).

difficult and the associated scale effects are not negligible.

3. NUMERICAL MODELING

In the previous sections, the background and summary of the work were presented, in this section, the CFD modeling and the theoretical foundations of the problem are presented.

3.1 Governing Equation

Navier-Stokes momentum equations fully describe turbulent flow and are solved simultaneously with the Continuity and the Energy equations. In this work, heat transfer and temperature changes are negligible. The averaged Continuity and Momentum equations can be written for incompressible flow in Cartesian coordinates and in tensor form as indicated by (1) and (2).

$$\frac{\partial \overline{u_i}}{\partial x_j} = 0 \tag{1}$$

$$\rho\left(\frac{\partial \overline{\mathbf{u_i}}}{\partial \mathbf{t}} + \overline{\mathbf{u}}_\mathbf{j}\frac{\partial \overline{\mathbf{u_i}}}{\partial \mathbf{x_j}}\right) = \overline{\mathbf{B}}_\mathbf{i} - \frac{\partial \overline{p}}{\partial \mathbf{x_i}} + \frac{\partial}{\partial \mathbf{x_j}}\left(\mu\left(\frac{\partial \mathbf{u_i}}{\partial \mathbf{x_j}}\right) - \rho \mathbf{u_i'u_j'}\right) \tag{2}$$

The turbulent velocity and pressure are described by superposition of two components, a nominal mean, and an oscillating part.

In these relations, the $\{\overline{\rho u_i' u_j'}\}$ is defined as the "Reynolds stress". The only difference between laminar and turbulent flow in this equation is the existence of the aforementioned term. Generally, this term is not physical stress; rather, it reflects the impact of inertia exchanges.

$$-\overline{\rho u_i' u_j'} = 2\mu_t S_{ij} - \frac{2}{3}\rho k \delta_{ij} \tag{3}$$

$$\bar{S}_{ij} = \frac{1}{2}\left(\frac{\partial \bar{u}_j}{\partial x_i} + \frac{\partial \bar{u}_i}{\partial x_j}\right) \tag{4}$$

In Eq. (3), δ is the Kronecker delta function; μt is the turbulent dynamic viscosity. To calculate this parameter, K-ε is used as the turbulent model which is a common practice for similar problems in research and industry (Tezdogan *et al.*, 2016).

There exist several ways to establish the inter-dependence between speed and pressure in the domain. In this study, the SIMPLE algorithm is used for this purpose (Löhner *et al.*, 2008).

3.2 Free SurfACE Modeling

For modeling the free surface, the volume of fluid (VOF) method is used. Figure 2 presents wave amplitudes on the free surface of the flow and Fig. 3 presents the value of volume fraction on the ship

hull for Froude number; 0.275. For example, a value of 0.6 in this figure indicates that the corresponding cell contains 60% water and 40% air.

In other to simulate the dynamic motion of the ship hull, Dynamic Fluid Body Interaction (DFBI) model is applied. This model involves solving the dynamic equations and the fluid governing equations simultaneously to compute the ship motion caused by fluid exciting forces. In this work, the following 4 degrees of freedom are considered: surge, roll, pitch and heave motions.

3.3 Wave Generation

Lin *et al.* (1999) developed the wave generating method using a mass source function. Choi *et al.* (2009) developed the method by using a momentum source instead of the mass source. Star-CCM software generates the wave inlet boundary base on the Choi and Yoon (2009) works.

The Join North Sea Wave Project (JONSWAP) spectra as a standardized wave spectra used to generate irregular waves (Hasselmann, 1973). According to DNV (2011), the average values for JONSWAP experiment data are $\gamma = 3.3$, $\sigma a = 0.07$, and $\sigma b = 0.09$

$$S_{PM}(\omega)=\frac{5}{16}\left(H_s^2\omega_p^4\right)\omega^{-5}\exp\left[-\frac{5}{4}\left(\frac{\omega_p}{\omega}\right)^4\right] \tag{5}$$

$$S_j(\omega)=A_\gamma S_{PM}(\omega)\gamma^{\exp\left[\frac{(\omega-\omega_p)^2}{2\sigma^2\omega^2}\right]} \tag{6}$$

$$A_g=1-0.287\mathrm{Ln}(g) \tag{7}$$

$$\sigma=\begin{cases}\sigma_a & \omega\le\omega_p\\ \sigma_b & \omega>\omega_p\end{cases} \tag{8}$$

3.4 Time-Step and CFL-Number

Choosing a time step for new problems is very important and can be difficult. When a large time step is used, some exchanges in momentum transport are not captured; this source causes numerical errors in the solution. Smaller values of the time-step cause longer computational time. Courant number is a good measurable index for this criterion, which is the ratio of time step to the mesh convection time scale.

$$CFL=\frac{\Delta t}{\Delta x\ /U} \tag{9}$$

Δx is cell dimension and U is flow speed on the cell. For numerical stability, the Courant number should be less than or equal to 1 in each cell.

In this study, the Courant number is calculated for each cell according to the flow properties and the time steps are selected such that the minimum encounter wave's period in irregular waves is divided into at least 100 steps for prediction of the ship response (ITTC., 2011). The time step has been considered fix value; $\Delta t = 0.01$. In the Star-CCM+ software control of the time-step base on a user-defined range of CFL, is available. This is a good facility when the body has not an oscillating behavior. Investigation in this study shows that considering a fix minimum value is useful because of frequent changes in the time-step lead to some increase of residual and calculation time.

3.5 Computational Setting

Two coordinate references are considered in the computational domain. Position of hull and mesh data are measured relative to a reference coordinate system and another moving coordinate system is fixed to the ship's center of gravity for measurement of the force, moment and motion of ship hull, as shown in Fig. 4.

The overall flow in the domain is affected by boundary condition dictates. To have a well-posed problem, all boundaries must have a specific condition. Initial and boundary conditions are usually defined according to the physics of the problem. The distance of the Ship hull from the boundary should be large enough so that the flow field around the ship hull remains unaffected. Figure 4 presents the selected boundary condition and Fig. 5 shows the required distances, as stated.

The ship hull condition is considered to have no-slip around the ship surface, so the velocity components on the hull surface are zero. Velocity inlet and the pressure outlet are utilized in calculations. Considering non-head sea ship motion simulation, the ship center line symmetry condition is not applicable. However, symmetry conditions can also be used at the domain sidewalls and horizontal upper and bottom boundaries. An alternative condition for the sidewalls is the inlet velocity condition.

3.6 Mesh Generation

According to the simulation of motion in irregular waves and a high amount of computation required, the overset mesh is used around the hull. The Overset mesh is a type of dynamic meshing in which the meshes move with the object on a fixed background of meshes. In this meshing method, mesh regeneration around the hull is not required in every step, and the overset mesh data is mapped into the background fixed meshes (DNV, 2011).

Considering ITTC (2011) and Kim *et al.* (2011) more than 180 grids points per wavelength and more than 20 cells in the vertical direction were used around the hull free surface over all the computational domain.

4. VERIFICATION

The process of verification and validation attempts to assess the accuracy and reliability within the CFD simulation. Verification and validation are extremely important when working with numerical simulations. Verification is defined as a process of assessing the numerical uncertainty of simulations, and when conditions permit, estimating the sign and magnitude of the simulation numerical error. The

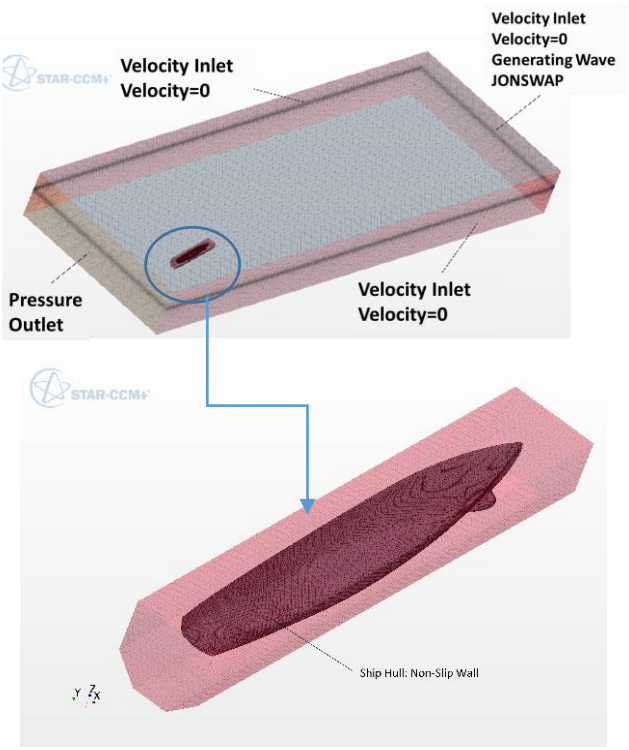

Fig. 4. Background and overset regions.

Table 3 Elements number and time steps size in the uncertainty study

Mesh Number		Cell Number		
		Background	Overset	Total
G1	Fine	7,704,928	4,223,591	11,928,519
G2	Medium	7,704,928	2,815,727	10,520,655
G3	Coarse	7,704,928	1,877,151	9,582,079
Time Step				
T1: $Te/2^{11}$		T2: $Te/2^{10}$		T3: $Te/2^{9}$

uncertainty estimates the numerical uncertainty and ambiguity in the simulation computations. Iterative and input parameter convergence studies are conducted using multiple solutions with systematic parameter as described on Stern *et al.* (2006).

It was assumed that the numerical error includes iterative convergence error (δI), grid-spacing convergence error (δG) and time-step convergence error (δT), which gives the following expressions for the simulation numerical error and uncertainty.

$$\boldsymbol{\delta_{SN} = \delta_I + \delta_G + \delta_T} \tag{10}$$

$$\boldsymbol{U_{SN}^2 = U_I^2 + U_G^2 + U_T^2} \tag{11}$$

As in similar studies like Stern *et al.* (2006), verification is carried out for the worst case of the simulation. In this work, at the heading angle of 10 degrees, motion and acceleration are severe, and it is considered as the worst case.

Iterative uncertainties in all trials are found to be very low when compared with grid and time step uncertainties. Therefore, it is assumed that $UI \approx 0$. The element number for the grid uncertainty and the time-step size for the convergence study are given in Table 3. Te is the encounter period. The results of the grid and time step convergence studies are given in Table 4 and 5. The number of elements in each overset grid is 1.5 times the previous grid as can be seen in Table 3, and the refinement ratio in grid convergence study is $rG=\sqrt{2}$ as it suggested in ITTC 7.5-03-01-01 (2008). The time-step is increased with a refinement ratio of 2, starting from $\Delta t=Te/2^{11}$. This value of refinement ratio for the time step leads to a sensitive change in solution results.

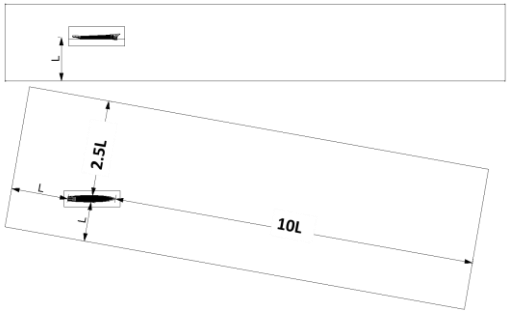

Fig. 5. Dimension of the computational domain for seakeeping analyses.

Table 4 Grid convergence study

Time-step =T1	Solutions			R_G	rG	CF			GCI		Sc
	S_G1	S_G2	S_G3			δ^*_G(%S1)	UG(%S1)	UGc(%S1)	UG(%S1)	UGc(%S1)	
RMS ROLL	0.2563	0.2545	0.2503	0.429	√2	-0.18%	3.24%	0.62%	0.7%	0.1%	0.2567
RMS PITCH	0.8927	0.8895	0.8816	0.405	√2	-0.11%	1.17%	0.19%	0.3%	0.1%	0.8937
RMS HEAVE	0.4703	0.4692	0.4559	0.083	√2	-0.21%	0.40%	0.19%	0.0%	0.0%	0.4713

Table 5 Time step convergence study

Grid = G1	Solutions			R_T	rT	CF			GCI		Sc
	S_T1	S_T2	S_T3			δ^*_T(%S1)	UG(%S1)	UGc(%S1)	UG(%S1)	UGc(%S1)	
RMS ROLL	0.2563	0.2552	0.2510	0.262	2	-0.78%	7.00%	6.31%	0.2%	0.0%	0.2583
RMS PITCH	0.8927	0.8895	0.8818	0.416	2	-0.95%	7.41%	4.62%	0.3%	0.1%	0.9012
RMS HEAVE	0.4703	0.4689	0.4650	0.359	2	-0.69%	1.21%	0.52%	0.2%	0.0%	0.4735

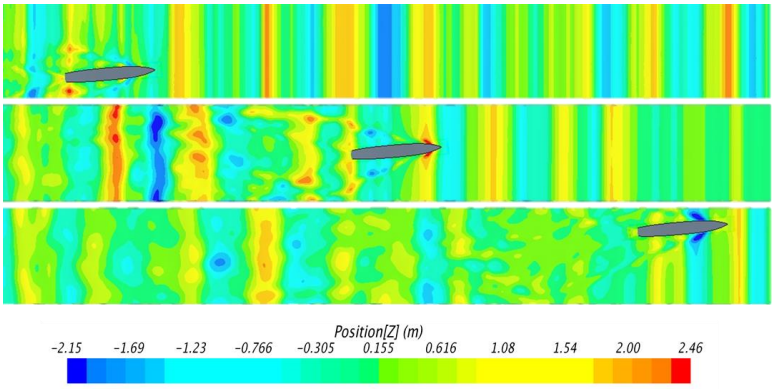

Fig. 6. Free surface wave contour top view.

For verification study, motion RMS of the roll, pitch, and heave is used as solution results. According to Stern *et al.* (2006), both verification procedures include Correction Factor (CF) and Grid Convergence Index (GCI) are performed. RG and RT are the convergence ratio. When these parameters are between 0 and 1, the monotonic convergence condition exists, and generalized RE (Richardson extrapolation) is used to estimate uncertainty. For more detail of the procedures, refer to Stern *et al.* (2006).

The grid uncertainties as a percentage of the grid 1 (G1) for roll, pitch and heave RMS are 3.24%, 1.17%, and 0.4%, respectively as shown in Table 4. The time-step uncertainties as a percentage of time-step 1 (T1), for roll, pitch and heave RMS are, 7.00%, 7.41%, and 1.21%, respectively as shown in

Table **5**. Mancini *et al.* (2018) also applied CF and GCI verification procedures on CFD modeling of DTMB5415 roll decay for a scaled model. In their work, roll motion grid uncertainty is 16.99% and time-step uncertainty is 0.88%. Also in similar work, Mohsin *et al.* (2019) grid uncertainty is 3.03%. Kianejad *et al.* (2019) applied CF and GCI verification procedures on CFD modeling of the full-scale container ship and minimum grid and time step uncertainty for roll motion are 3.33% and 1.86% respectively.

5. RESULTS AND DISCUSSION

According to computational domain dimensions, 150 seconds is required to travel the length of the domain. In this work by using a parallel processing computer with 64 x 2.5GHz core and 128GB RAM, solving time lasted for 168 hours. In this study, only 75 seconds of the time was used for post-processing to avoid walls effects due to domain end nearing.

Figures 6 and 7 present the ship sailing in the start, mid and end of the computational domain. At first, waves are propagated along with the domain, and the ship starts to move. Using the stated velocity inlet boundary condition prevents wave reflections at the side walls. As shown in Fig. 6 and 7, when the ship reaches the end of the domain, the waves are not reflected. The disturbance wake behind the ship is due to the interaction between sea waves and hull generated waves. In roll motion, positive roll angle corresponds to starboard, in pitch motion, the positive pitch angle is by fore and in heave motion, upward is positive.

In Fig. 8 through 10, Roll, Pitch, and Heave motion time histories for 75 seconds are presented. In the roll motion, the average value is zero, but in pitch, the average value is equal to initial trim, which is according to hydrostatic equilibrium condition. In

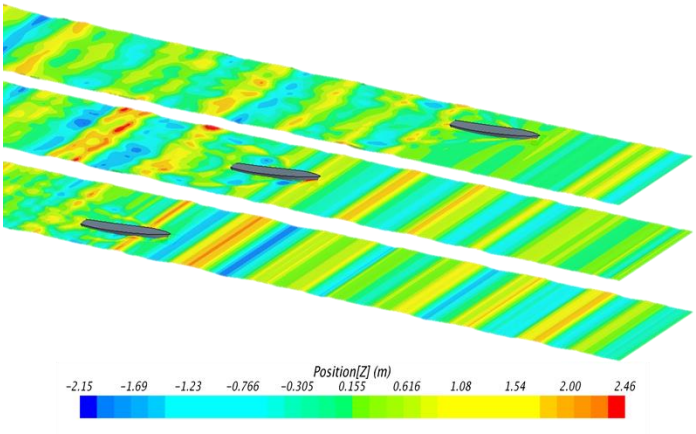

Fig. 7. Free surface wave contour isometric view.

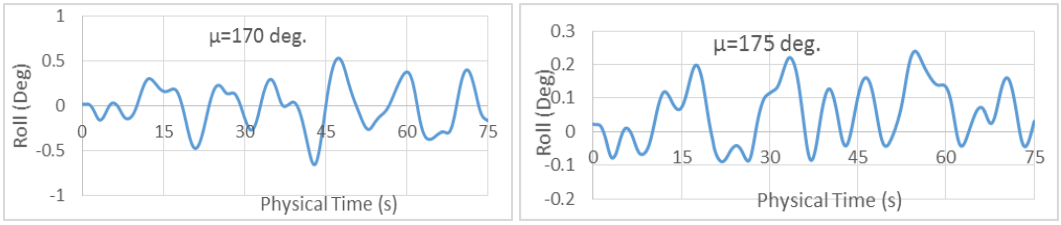

Fig. 8. Roll motion time history.

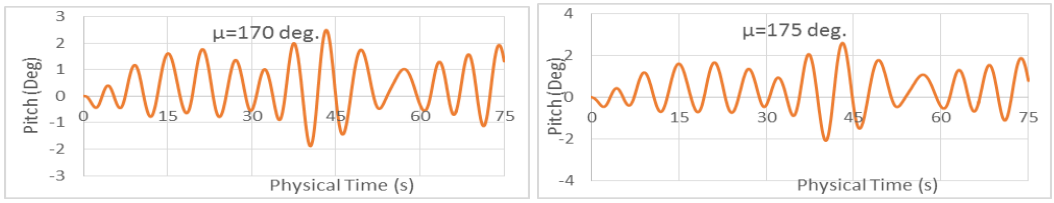

Fig. 9. Pitch motion time history.

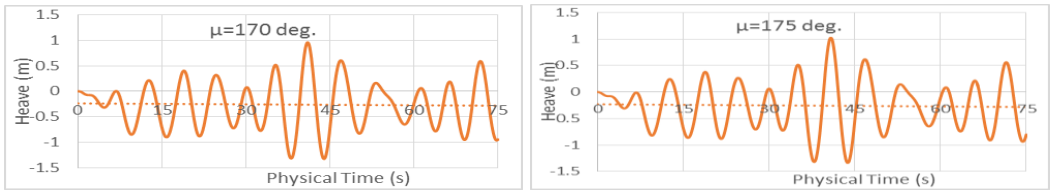

Fig. 10. Heave motion time history.

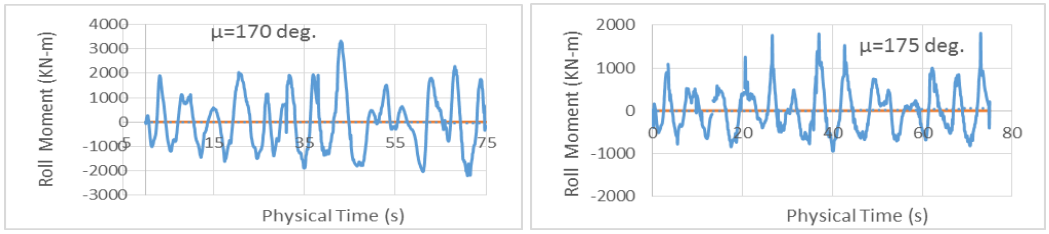

Fig. 11. Roll moment time history.

heave motion, the average value equals to zero point sinkage of the ship at the aft perpendicular. The 5 degrees increase in heading angle causes a little change in the vertical motion and causes more effects on the roll motion.

In CFD simulation; forces can be obtained by integration of pressure on ship hull surface and moments which is calculated in accordance with the references point. In Fig. 11, the roll exciting moment is presented. Comparing these results with the roll motion illustrated in Fig. 8, it is evident that all the forces do not result in roll motion, and the frequency of oscillation is quite important. Figure 14 shows the roll moment energy spectrum. The

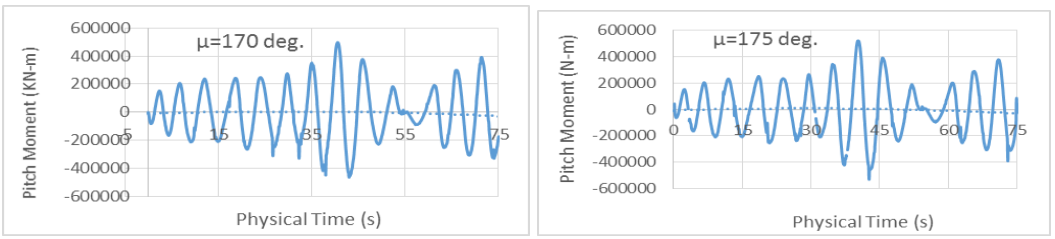

Fig. 12. Pitch exiting moment time history.

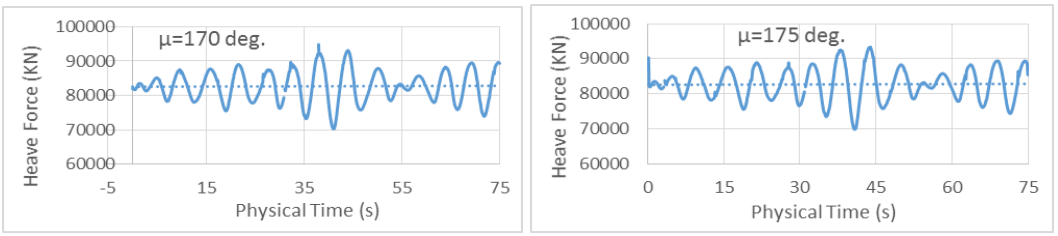

Fig. 13. Heave exciting force time history.

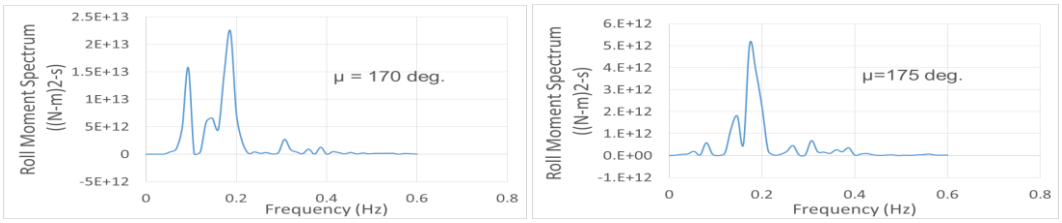

Fig. 14. Roll Moment spectrum.

exciting moment amplitude or energy peak occurs in frequencies of 0.1 Hz and 0.18 Hz. By comparing this result with the motion spectrum, as shown in Fig. 15, only the first peak (0.1Hz) results in roll motion. This frequency is in accordance with the natural frequency of the ship hull.

The linear strip theory is used to calculate the coupled heave and pitch response of the vessel. The roll response is calculated using linear roll damping theory. Fundamental to strip theory is the calculation of sections hydrodynamic properties. Conformal mappings are transformations which map arbitrary shapes in one plane to circles in another plane. One of the most practical and useful transformations is the Lewis mapping, which maps a wide range of ship-like sections to the unit circle. The solution of the potential flow formulation for a unit circle may then be applied to an arbitrary hull form. In this study, motion response in similar condition was calculated by the strip theory method, and results were presented.

Figure 15 through 20 present the energy spectrum of the ship motions. There is good conformation in the pitch and the heave motions but, in the roll motion, some deviation is considerable. Table 6 presents the RMS values of the indicated motions obtained from the CFD and the strip theory calculations. Increasing the heading angle produces more nonlinearity viscous effects, and as a result, the strip theory and the CFD results for the roll motion get away from each other. Linear roll damping theory used constant damping coefficient and second order differential equation is solved such as that describing a forced spring, mass, and damper system. In reality, hydrodynamic coefficients, especially damping coefficient are not linear, and it changes by dynamic of motion. Therefore, the applied linear roll damping theory cannot accurately predict the damping and exciting forces. Considering the roll moment spectrum in Fig. 14, in heading angle; μ=170 deg.; both CFD and Strip theory method can compute the second energy peak (~0.18Hz) and the first energy peak (~0.1Hz) only occurred in CFD. As a result, the motion spectrum in Fig. 15 show that both CFD and Strip theory have the same pick in 0.18 Hz but in 0.1Hz only CFD method computed the energy peak in roll motion. In μ=175, the heading angle gets closer to the head sea condition, and the first energy peak (~0.1Hz) decreased, so the strip theory and the CFD results for the roll motion get closer to each other.

Table 6 motion RMS values

Parameter	Heading angle (μ)	CFD	Strip theory
Roll RMS (m)	170 deg.	0.252	0.092
	175 deg.	0.087	0.092
Pitch RMS (m)	170 deg.	0.880	0.812
	175 deg.	0.903	0.798
Heave RMS (m)	170 deg.	0.460	0.420
	175 deg.	0.461	0.418

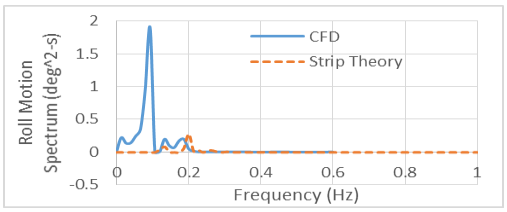

Fig. 15. Roll Motion spectrum (μ=170 deg.).

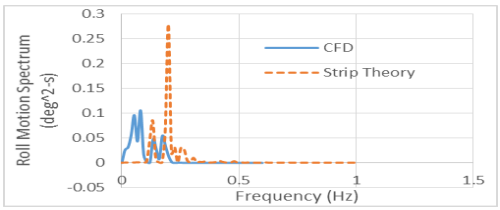

Fig. 16. Roll Motion spectrum (μ=175 deg.).

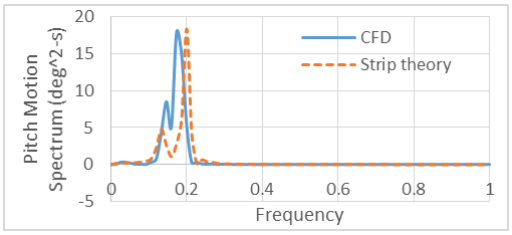

Fig. 17. Pitch Motion spectrum (μ=170 deg.).

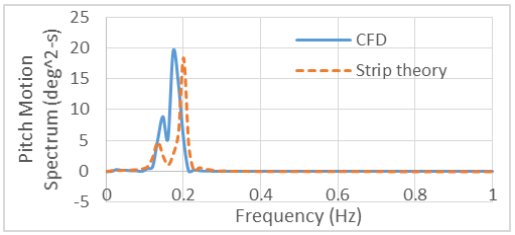

Fig. 18. Pitch Motion spectrum (μ=175 deg.).

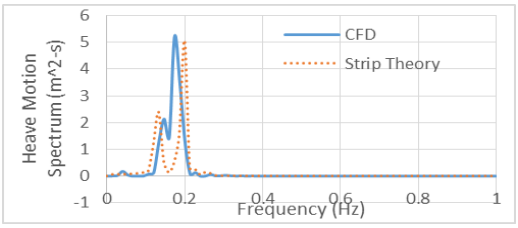

Fig. 19. Heave Motion spectrum (μ=170 deg.).

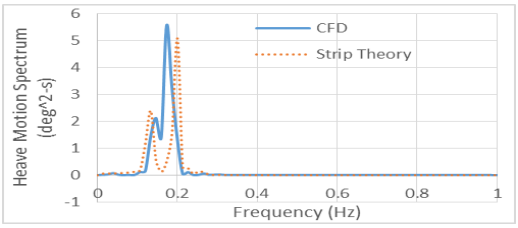

Fig. 20. Heave Motion spectrum (μ=175 deg.).

6. CONCLUSIONS AND FUTURE WORKS

This paper presents a new approach for time-domain 4DOF CFD simulation of full-scale ship model using the unsteady Reynolds-Averaged Navier–Stokes method. Due to the lack of appropriate experimental data for validation of the results, the linear strip theory method has been used to verify the CFD obtained results.

In this work, a CFD simulation of the ship sailing in seaway using a commercial RANS solver, Star-CCM 10.06 was presented. The novelty of the paper was full-scale four degrees of freedom simulation of DTMB 5415 ship motion in irregular oblique sea waves. This research will be extended to subscale test experiments for more definite validation of the results. However, the computational domain developed in this work is virtually similar to a large towing tank.

Irregular waves were generated on the inlet boundary and propagated along with the computational domain while the ship moved in the domain. The ship has 4DOF in the surge, roll, pitch and heave directions. In the type of modeling used here, Non-head sea waves or oblique waves can be generated for simulation purposes. Irregular waves were generated using JONSWAP spectra and wave parameters including significant height and modal periods. These parameters were selected in accordance with the desired sea state. A rectangular computational domain was established for the simulation, and the deflection angle between the domain and the ship's longitudinal axis was considered so that a selected heading angle was formed.

The arrangement of the ship and computational domain presented in Fig. 2 is very important in simulation. Waves should propagate parallel to the computational domain sides. Otherwise, waves will return from boundary to domain and will disturb the free surface pattern.

The overset meshing procedure was used around the hull. In this meshing method, mesh regeneration around the hull was not required in every step. Instead, the overset mesh data was mapped into the background fixed meshes.

In reality, hydrodynamic coefficients, especially damping coefficient are not linear and it changes by dynamic of motion. Considering the roll moment and motion spectrum results, only the CFD method can compute all energy peaks. When the heading angle gets closer to the head sea condition results of the strip theory and CFD method for the roll motion get closer to each other.

This paper has provided useful starting point dynamic simulation for performance evaluation and some appertaining control system design, especially for the roll motion. One of the main difficulties in prediction of the nonlinear roll motion is decoupling the roll equations and estimating the roll coefficients. The proposed method can be used to calculate the damping coefficients of full-scale vessels without limitations involved when scale factors and experimental test models are used. CFD simulation can provide thorough data concerning performance characteristics of ships, and in that respect, it is useful for researchers who study

motion control of ships to obtain the effective modal frequencies.

FUNDING

This research received no specific grant from any funding agency in the public, commercial, or not-for-profit sectors.

REFERENCES

Alessandrini, B., Ferrant, P. and L. Gentaz (2008). Numerical simulation of ship seakeeping by the SWENSE approach, *Proceedings of the 10th International Ship Stability Workshop*, Nantes, France.

Bhushan, S., T. Xing, P. Carrica and F. Stern (2007-Aug.). Full-scale Model URANS/DES simulations for Athena R/V resistance, powering, and motions. *Proceedings Ninth International Conference on Numerical Ship Hydrodynamics*. August 5–8. Ann Arbor, MI.

Choi, J. and S. B. Yoon (2009). Numerical simulations using momentum source wave-maker applied to RANS equation model. *Coastal Engineering* 56(10), 1043-1060.

DNV. (2011). Modeling and Analysis of Marine Operations. (Vol. DNV-RP-H103).

Gocke, M. and O. Kinaci (2018). Numerical simulations of free roll decay of DTMB 5415. *Ocean Engineering* 159, 539-551.

Gui, L., J. Longo, B. Metcalf, J. Shao and F. Stern (2002). Force, moment and wave pattern for surface combatant in regular head waves. *Springer-Verlag, Experiments in fluid* 32, 27-36.

Hanninen, S. and T. Mikkola (2006). Computation of ship-hull flows at model and full-scale Reynolds numbers. *Proceedings of Numerical Ship Hydrodynamics Seminar*, Maritime Institute of Finland, Turku.

Hasselmann, K. (1973). Measurements of wind-wave growth and swell decay during the joint North Sea wave project (JONSWAP) (Vol. 12). Hamburg, Deutsches Hydrographic Institute

Hino, T. (2005). CFD Workshop Tokyo. *Proceedings of National Maritime Research Institute Tokyo*, Japan.

ITTC. (2011). Recommended Procedures and Guidelines, Practical Guidelines for Ship CFD applications, Recommend Procedures. 7.5-03-02-3.

ITTC. (2008) Uncertainty Analysis in CFD Verification and Validation Methodology and Procedures. 7.5-03-01-01.

Kianejad, S. S., H. Enshaei, J. Duffy and N. Ansarifard (2019). Prediction of a ship roll added mass moment of inertia using numerical simulation. *Ocean Engineering* 173, 77-89

Kim, S. P. and H. H. Lee (2011). Fully nonlinear seakeeping analysis based on CFD simulations. *Proceedings of the 21st International Offshore and Polar Engineering Conference*. Hawaii, USA, 970–974.

Kodama, Y., H. Takeshi, M. Hinatsu, T. Hino, S. Uto, N. Hirata and S. Murashige (1994). CFD Workshop. *Proceedings of the 1994 CFD Workshop*. Ship Research Institute, Japan.

Larsson, L., F. Stern and V. Bertram (2003). Benchmarking of Computational Fluid Dynamics for Ship Flows. *Journal of Ship Research* 47(1), 63-81.

Lin, P. and P. L. F. Liu (1999). Internal wave-maker for Navier-Stokes equations models. *Journal of Waterway, Port, Coastal and Ocean Engineering* 125(4), 207.

Löhner, R. (2008). *Applied Computational Fluid Dynamics Techniques*. ISBN: 978-0-470-51907-3, Second Edition, John Wiley & Sons, Ltd. 2008

Mancini, S., E. Begovic, A. Day and A. Incecik (2018). Verification and validation of numerical modelling of DTMB 5415 roll decay. *Ocean Engineering* 162, 209- 223.

Mohsin, A. R., S. Nallayarasu and S. K. Bhattacharyya (2019). Numerical prediction of roll damping of ships with and without bilge keel. *Ocean Engineering* 179, 226-245.

Pierson, J. W. J. and L. Moskowitz (1963). A Proposed Spectral Form for Fully Developed Wind Seas Based on the Similarity Theory of S. A. Kitaigorodskii. *Journal of Geophysical Research* 69(24), 5181-5190.

Simonsen, C. D. and F. Stern (2013). CFD simulation of KCS sailing irregular head waves. *Journal of Marine Science and Technology* 18(4), 435-459.

Stern, F., R. Wilson and J. Shao (2006). Quantitative V&V of CFD simulations and certification of CFD codes. *International journal for numerical methods in fluids* 50, 1335-1355.

Tezdogan, T., Y. Demirel, P. Kellett, M. Khorasanchi, , A. Incecik and O. Turan (2015). Full-scale unsteady RANS CFD simulations of ship behavior and performance in head seas due to slow steaming. *Ocean Engineering* 97, 186-206

Tezdogan, T., A. Incecik and O. Turan (2016). Full-scale unsteady RANS simulations of vertical ship motions in shallow water. *Ocean Engineering* 123, 131-145

Toxopeusa, S., F. Walreeb and R. Allmannba (2011) Maneuvering and Seakeeping Tests for 5415M. *Maritime Research Institute (MARIN)*, Delft University of Technology.